

HUPD-9217  
December 1992

# Measuring the Beam Polarizations and the Luminosity at Photon–Photon Colliders

Yoshiaki YASUI, Isamu WATANABE\* †, Jiro KODAIRA and Ichita ENDO

*Department of Physics, Hiroshima University  
1-3 Kagami-yama, Higashi-Hiroshima 724 JAPAN*

## ABSTRACT

We present methods to measure the beam polarizations and the luminosity of  $\gamma\gamma$  colliders at TeV energy scale. The beam polarizations of a  $\gamma\gamma$  collider can easily be monitored by comparing the numbers of events of the processes  $\gamma\gamma \rightarrow \ell^+\ell^-$  and  $\gamma\gamma \rightarrow W^+W^-$ , where  $\ell$  means  $e$  or  $\mu$ . The luminosity of a  $\gamma\gamma$  collider is also measurable by the event rate of  $W$  boson pair productions and the light lepton pair productions.

---

\* Fellow of the Japan Society for the Promotion of Science for Japanese Junior Scientists. Work supported in part by the Grant-in-Aid for Scientific Research from the Ministry of Education, Science and Culture of Japan No. 040005.

† Address after Apr. 1, 1993: Theory group, KEK, Tsukuba, Ibaraki 305, JAPAN.

## §1 . Introduction

Photon–photon colliders<sup>[1,2]</sup> are seriously considered as one of the interesting options to upgrade future linear  $e^+e^-$  colliders. A lot of authors have reported on the advantages of a  $\gamma\gamma$  collider from various physical viewpoints.<sup>[3,4,5]</sup> For instance, the most interesting aspect in the  $\gamma\gamma$  process at TeV energy scale may be Higgs boson productions on the mass pole via loop effects. The signal of Higgs boson productions at a photon–photon collider will be much clearer than those at  $e^+e^-$  colliders or hadron colliders, and a  $\gamma\gamma$  collider is accessible to Higgs boson with heavier mass than the underlying  $e^+e^-$  colliders be.<sup>[3]</sup> As seen in this example, the photon–photon colliders will be necessary and important facilities in the future high energy physics.

At a photon–photon collider, the photon beams are generated through the backward Compton scattering of the laser beams by the high energy electron beams which are supplied by the underlying  $e^+e^-$  ( $e^-e^-$ ) collider. The theoretical studies on the beam conversion from electron into photon<sup>[1,2,6]</sup> and on the photon beam collision<sup>[1,2]</sup> have been performed by many authors. These theoretical estimates must be verified experimentally and the luminosity and the beam polarizations should be measured by actual observations. Note that both the luminosity and the polarization depend on the details of the beam overlap at the interaction point and the knowledge of the electron and laser polarization is not sufficient to determine the relevant parameters of the photon-photon system. However the ways to measure the luminosity and the beam polarizations are *not* trivial at photon–photon colliders. Unlike the  $e^+e^-$  collisions, there is no process which has a huge cross section, like Bhabha scattering, in  $\gamma\gamma$  collisions. There is an idea that the luminosity could be measured by the processes  $\gamma\gamma \rightarrow e^+e^-\mu^+\mu^-$  or  $e^+e^-e^+e^-$ , because of the constant total cross sections in the colliding energy.<sup>[7]</sup> Unfortunately, such a claim is not realistic, since these *total* cross sections are maintained by the collinear singularities: The typical muon production angle in the process  $\gamma\gamma \rightarrow e^+e^-\mu^+\mu^-$  turns out to be given by the ratio of the muon mass to the photon energy, and it is less than  $10^{-3}$  rad for the photon energy greater than 100 GeV. Electrons will be produced much more collinearly. Such collinear leptons will never be observed by a realistic detector which must evade the dumped bunches.

In this paper we present a convenient technique to measure the circular polar-

ization of the photon beams, as well as a method of the luminosity measurement at future photon–photon colliders. This paper is organized as follows. In §2 we review the theoretical estimates on the photon beam polarizations and the  $\gamma\gamma$  luminosity. We derive the cross sections of lepton pair productions and  $W$  boson pair productions in §3. The ideas of our new techniques to measure the photon beam polarization and the collider luminosity are described in §4 and §5, respectively. §6 gives some comments on the applications of our methods in the actual experimental situations.

## §2 . Theories on Photon Beam Generations and Collisions

To fix our notation, we first review the theoretical aspects of photon beam generations and photon–photon collisions.

The back-scattered photon spectrum can be given by the differential Compton cross section  $\sigma_c$ ,<sup>[2]</sup>

$$\begin{aligned} \mathcal{D}_\gamma(y) &\equiv \frac{1}{\sigma_c} \frac{d\sigma_c}{dy} \\ &= \frac{\sigma'_0 + P_e P_L \sigma'_1}{\sigma_0 + P_e P_L \sigma_1} , \end{aligned} \quad (1)$$

where,

$$\begin{aligned} \sigma'_0 &\equiv 2 \left( 1 - y + \frac{1}{1-y} - 4r(1-r) \right) , \\ \sigma'_1 &\equiv -2rx(2-y)(2r-1) , \\ \sigma_0 &\equiv 2 \left( 1 - \frac{4}{x} - \frac{8}{x^2} \right) \log(x+1) + 1 + \frac{16}{x} - \frac{1}{(x+1)^2} , \\ \sigma_1 &\equiv 2 \left( 1 + \frac{2}{x} \right) \log(x+1) - 5 + \frac{2}{x+1} - \frac{1}{(x+1)^2} . \end{aligned} \quad (2)$$

Here  $y$  is the ratio of the scattered photon energy  $E_\gamma$  to the electron beam energy  $E_e$ , *i.e.*  $y \equiv E_\gamma/E_e$ ;  $x$  is the squared ratio of the total energy of the Compton scattering in the center-of-mass system to the electron mass  $m_e$ ,  $x \equiv 4E_e\omega/m_e^2$ , where  $\omega$  is the laser light energy;  $r \equiv y/x(1-y)$ ;  $P_e$  and  $P_L$  denote the polarizations of the beam electron and the laser photon, respectively. Note here that each of the  $P_e$  and  $P_\gamma$  is

normalized to  $+1$  ( $-1$ ) corresponding to the 100% positive (negative) polarization. We assumed the optimum value of  $x$ ,  $x = 2 + 2\sqrt{2}$ <sup>[1]</sup> in the subsequent discussions. The value of  $y$  is restricted in the range between 0 and  $y_m \equiv x/(1+x) \simeq 0.828$ . The polarization distribution of the produced photon beam  $P(y)$  is also calculated.<sup>[2]</sup>

$$P(y) = \frac{P_e rx [ 1 + (1-y)(2r-1)^2 ] - P_L ( 1 - y + \frac{1}{1-y} ) (2r-1)}{1 - y + \frac{1}{1-y} - 4r(1-r) - P_e P_L rx (2-y)(2r-1)} . \quad (3)$$

Typical photon beam spectrum and polarization distribution are plotted in Fig. 1 for several values of  $P_e$ . As seen in this figure, the electron beam polarization  $P_e$  and the laser photon polarization  $P_L$  should be controlled such that  $P_e P_L \simeq -1$ , to improve the monochromaticity of the produced photon beam. It is believed that the laser beam can be polarized easily and almost completely, since the necessary laser light is visible ( $E_e \lesssim 195$  GeV) or near infrared. A technology to produce a highly polarized energetic electron beam is now developing successfully.<sup>[8]</sup> *The fact that the photon beams are polarized will be an essential feature of the  $\gamma\gamma$  colliders.* Under such a polarization set-up, *i.e.*  $P_e P_L \simeq -1$ , the typical photon beam energy is roughly 0.8 times of the electron beam energy, and the absolute value of  $P(y)$  at large  $y$  is almost uniform and unity.

To avoid complicated discussions on the beam conversion kinematics and collider designs, we simply evaluate the luminosity distribution as,

$$\frac{1}{\mathcal{L}_{\gamma\gamma}} \frac{d^2 \mathcal{L}_{\gamma\gamma}}{dy_1 dy_2} = \mathcal{D}_\gamma(y_1) \mathcal{D}_\gamma(y_2) , \quad (4)$$

or,

$$\frac{1}{\mathcal{L}_{\gamma\gamma}} \frac{d^2 \mathcal{L}_{\gamma\gamma}}{dz d\eta} = 2z \mathcal{D}_\gamma(ze^{+\eta}) \mathcal{D}_\gamma(ze^{-\eta}) , \quad (5)$$

where  $y_1$  and  $y_2$  are the energy ratios of the produced photons to the beam electrons which are accelerated to the opposite direction 1 and 2;  $z$  is the fraction of the photon–photon collision energy  $\sqrt{s}$  to the sum of the electron beam energies, *i.e.*  $z \equiv \sqrt{y_1 y_2} = \sqrt{s}/2E_e$ ;  $\eta$  is the  $\gamma\gamma$  rapidity in the laboratory system,  $\eta \equiv \log \sqrt{y_1/y_2}$ . Here  $z$  runs over the region between 0 and  $y_m$ , and then  $\eta$  is restricted to be  $-\log(y_m/z) \leq \eta \leq +\log(y_m/z)$ . It is assumed that the back-scattered photons collide each other just after the Compton conversion.<sup>1)</sup> A contour plot of the luminosity distribution,

<sup>1)</sup> If we take into account the separation between the conversion point and the interaction point, the effect of the finite angle of Compton scatterings would result in an improvement of the beam monochromaticity and a suppression of the luminosity.<sup>[1,2]</sup>

as well as the partially integrated luminosity distributions, is illustrated in Fig. 2 for the ideal polarization case  $P_e P_L = -1$ . A good peak is observed at the corner of high  $z$  value. The peak in  $d\mathcal{L}_{\gamma\gamma}/dz$  distribution is located at  $z \simeq 0.788$ .

The events at low  $z$  values should be discarded to avoid possible miss-identifications of the processes. For example,  $\gamma\gamma \rightarrow W^+W^- \rightarrow \ell^+\nu_\ell\ell^-\bar{\nu}_\ell$  or  $\gamma\gamma \rightarrow \ell^+\ell^- + (\text{collinear } \ell^+\ell^-)$  may be miss-identified as low  $z$  events of  $\gamma\gamma \rightarrow \ell^+\ell^-$ , if the imbalance of transverse momenta of detected particles is small. Therefore we introduce a cut on  $z$  as  $z \geq z_{\text{cut}}$  to extract good events. In Table 1 and Fig. 3(a) we give the luminosity fraction  $\mathcal{F}r$  integrated over  $z_{\text{cut}} \leq z \leq y_m$ ,

$$\mathcal{F}r(z_{\text{cut}}) \equiv \frac{1}{\mathcal{L}_{\gamma\gamma}} \int_{z_{\text{cut}}}^{y_m} dz \frac{d\mathcal{L}_{\gamma\gamma}}{dz} , \quad (6)$$

for two cases of  $P_e = +1.0$ ,  $P_L = -1.0$  and  $P_e = +0.8$ ,  $P_L = -1.0$ . If we adopt 0.75 as a value of  $z_{\text{cut}}$ ,  $\mathcal{F}r(0.75)$  is 16% for the ideal electron beam polarization  $P_e = +1.0$ , or is 14% for a conservative value of  $P_e = +0.8$ . Due to the small, but finite, scattering angles of Compton back-scatterings at the beam conversion points which would be distant from the interaction point, the effective luminosity of a  $\gamma\gamma$  collider will be decreased from those of underlying  $e^+e^-$  colliders, though a photon–photon collider is free from the beam–beam interaction effect which essentially limits the luminosity of  $e^+e^-$  colliders. Forthcoming linear  $e^+e^-$  colliders considered are at the energy scale between 0.3 and 2.0 TeV, and with the luminosity around 10 or 100  $\text{fb}^{-1}$  a Snowmass year ( $10^7$  s).<sup>[9]</sup> Then we focus our further discussions on future photon–photon colliders whose center-of-mass energy is between 0.2 and 2.0 TeV and whose luminosity above  $z_{\text{cut}}$  is roughly  $1 \text{ fb}^{-1}$  per Snowmass year ( $10^{32} \text{ cm}^{-2} \text{ s}^{-1}$ ).

If a beam photon is at the maximum energy fraction  $y = y_m$ , then the beam photon polarization  $P$  is +1 or -1 according to the laser polarization  $P_L$  which is now assumed to be  $\pm 1$ , just as seen in Fig. 1(b),

$$\begin{aligned} P_L = -1 &\quad \rightarrow \quad P(y_m) = +1 , \\ P_L = +1 &\quad \rightarrow \quad P(y_m) = -1 . \end{aligned} \quad (7)$$

If two photons of both beams are in this limit, the product of  $\gamma$  polarizations is pure and ideal, *i.e.*  $P_1 P_2 = \pm 1$ , where  $P_1$  and  $P_2$  are the photon polarizations of beam 1 and 2, respectively. On the other hand, the worst combination of  $P_1$  and  $P_2$

above  $z_{\text{cut}}$ ,  $\mathcal{W}r(z_{\text{cut}})$ , comes from the case that one photon has the maximum energy fraction  $y = y_m$  and the other has the minimum  $y = z_{\text{cut}}^2/y_m$ ,

$$\begin{aligned}\mathcal{W}r(z_{\text{cut}}) &\equiv P(y_m) P(z_{\text{cut}}^2/y_m) , \\ &= \pm P(z_{\text{cut}}^2/y_m) .\end{aligned}\quad (8)$$

The average of the polarization product  $P_1 P_2$  over the whole region of  $z \geq z_{\text{cut}}$ ,  $\mathcal{A}v(z_{\text{cut}})$ , can be obtained as follows,

$$\mathcal{A}v(z_{\text{cut}}) \equiv \frac{1}{\mathcal{L}_{\gamma\gamma}} \int_{z_{\text{cut}}}^{y_m} dz \frac{d\mathcal{L}_{\gamma\gamma}}{dz} P_1 P_2 . \quad (9)$$

In Table 1 and Fig. 3(b) we also show  $\mathcal{A}v$  and  $\mathcal{W}r$  versus  $z_{\text{cut}}$ . If we choose  $z_{\text{cut}} = 0.75$ , the mean polarization product  $\mathcal{A}v$  reaches to  $\pm 97\%$  for the ideal electron polarization  $P_e = \pm 1.0$ , and  $\pm 85\%$  for a conservative electron polarization  $P_e = \pm 0.8$ . Even in the worst polarization case  $\mathcal{W}r(0.75)$ , it drops down only to  $\pm 81\%$  and  $\pm 59\%$  corresponding to  $P_e = \pm 1.0$  and  $\pm 0.8$ , respectively. Therefore two colliding photon beams can be regarded as almost uniformly polarized above the appropriate  $z_{\text{cut}}$  value.

### §3 . Lepton and $W$ Pair Productions at $\gamma\gamma$ Colliders

To avoid the theoretical ambiguities the luminosity and the beam polarizations will be monitored by the processes which occur at the tree-level. And the processes with only two final particles will earn greater event rates than the ones with many final particles. Therefore we concentrate in the processes of the light lepton pair production  $\gamma\gamma \rightarrow \ell^+ \ell^-$ , where  $\ell$  means  $e$  or  $\mu$ , and the  $W$  boson pair production  $\gamma\gamma \rightarrow W^+ W^-$ . Of course, there are some possibilities that new physics contributes to these cross sections. Anomalous  $\gamma WW$  or  $\gamma\gamma WW$  couplings may change the  $W$  pair production cross section. Even in the standard model, the Higgs boson pole may increase the  $W$  boson production rate in the collisions of photons with the same sign helicities. Such possibilities of new physics must be checked by detailed analyses. In the present paper, however, we confine ourselves to the standard theory because the effects of the new physics are to be learned by analyzing *the actual events* for which high statistics measurement is possible in a reasonable period.<sup>[4]</sup>

As mentioned in the previous section the photon beams are essentially polarized at  $\gamma\gamma$  colliders. Then we *have to* take into account the beam polarizations in our calculations of the cross sections.

The differential cross section of the process  $\gamma\gamma \rightarrow \ell^+\ell^-$  with the photon helicities fixed can easily be evaluated at the tree-level.<sup>[10]</sup>

$$\begin{aligned} \frac{d\sigma^{(\pm,\pm)}(\gamma\gamma \rightarrow \ell^+\ell^-)}{d\cos\theta} &= \frac{4\pi\alpha^2}{s} \frac{\beta(1-\beta^4)}{(1-\beta^2\cos^2\theta)^2} , \\ \frac{d\sigma^{(\pm,\mp)}(\gamma\gamma \rightarrow \ell^+\ell^-)}{d\cos\theta} &= \frac{4\pi\alpha^2}{s} \frac{\beta^3(1-\cos^2\theta)\{2-\beta^2(1-\cos^2\theta)\}}{(1-\beta^2\cos^2\theta)^2} . \end{aligned} \quad (10)$$

Here  $\beta$  and  $\theta$  are the velocity and the scattering angle of a final charged lepton  $\ell$ , and  $(\pm, \pm)$  or  $(\pm, \mp)$  represents that the helicities of two colliding photon are the same or the opposite sign. Note here that  $\beta$  and  $\theta$  adopted here are defined in the center-of-mass system of the colliding photons, not in the laboratory frame. The fine structure constant  $\alpha$  in Eq. (10) should be defined at the energy scale of  $\gamma\gamma$  collisions and has a value about 1/128. For the light leptons, Eq. (10) is characterized by strong peaks in the very forward and backward region caused by the collinear singularity. Especially in  $(\pm, \pm)$  helicity set, the massless lepton can only be emitted at  $\cos\theta = \pm 1$ .

Such collinear leptons cannot be observed in an actual experimental situation. Therefore, we introduce an angle cut  $|\cos\theta| \leq a$  and integrate Eq. (10) to obtain the relevant cross section.

$$\begin{aligned} \sigma_{|\cos\theta|\leq a}^{(\pm,\pm)}(\gamma\gamma \rightarrow \ell^+\ell^-) &= \frac{4\pi\alpha^2}{s} (1-\beta^4) \left[ \frac{1}{2} \log \frac{1+a\beta}{1-a\beta} + \frac{a\beta}{1-(a\beta)^2} \right] , \\ \sigma_{|\cos\theta|\leq a}^{(\pm,\mp)}(\gamma\gamma \rightarrow \ell^+\ell^-) &= \frac{4\pi\alpha^2}{s} \left[ \frac{5-\beta^4}{2} \log \frac{1+a\beta}{1-a\beta} \right. \\ &\quad \left. - a\beta \left\{ 2 + \frac{(1-\beta^2)(3-\beta^2)}{1-(a\beta)^2} \right\} \right] . \end{aligned} \quad (11)$$

It is possible to make a convolution of the above cross section with the photon beam spectra. However, a photon beam spectrum depends on the details of the conversion mechanics, *e.g.* the distance between the conversion point and the interaction point, the Compton scattering angle, the size and the shape of the electron bunch. And the beam spectrum is an object which *should be determined* by an actual observation experimentally. Therefore we do *not* make such a convolution, and discuss in the  $\gamma\gamma$  C. M. system in each collision. We present the cross sections with an angle cut

$a = 0.9$  versus  $\sqrt{s}$  for both helicity combinations in Fig. 5, and similar ones without any angle cut in Fig. 4 for comparison. One can observe a dramatic role of the angle cut in these two figures. As seen in Fig. 5,  $e$  and  $\mu$  productions with the photon helicity  $(\pm, \pm)$  are negligible for an integrated luminosity around  $1 \text{ fb}^{-1}$ . On the other hand, a large number of lepton pairs will be created by  $(\pm, \mp)$  photon beam collisions. It is worth noting that the production cross section of a lepton pair are greater than those of a quark pair. For quark pair productions, a color factor 3 and a charge factor (charge)<sup>4</sup> should be multiplied to R. H. S. of Eqs. (10) and (11), rather than  $3 \times (\text{charge})^2$  in  $e^+e^-$  collisions.

The cross section of the process  $\gamma\gamma \rightarrow W^+W^-$  shows a different dependence on the photon helicities. The differential cross sections and the cross sections with the angle cut for both helicity combinations are as follows<sup>[11]</sup>

$$\begin{aligned} \frac{d\sigma^{(\pm, \pm)}(\gamma\gamma \rightarrow W^+W^-)}{d\cos\theta} &= \frac{2\pi\alpha^2}{s} \frac{\beta_W(3 + \beta_W^2)(1 + 3\beta_W^2)}{(1 - \beta_W^2 \cos^2\theta)^2} , \\ \frac{d\sigma^{(\pm, \mp)}(\gamma\gamma \rightarrow W^+W^-)}{d\cos\theta} &= \frac{2\pi\alpha^2}{s} \beta_W \left[ 3 - \frac{22 - 6\beta_W^2}{1 - \beta_W^2 \cos^2\theta} \right. \\ &\quad \left. + \frac{(5 - \beta_W^2)(7 - 3\beta_W^2)}{(1 - \beta_W^2 \cos^2\theta)^2} \right] , \end{aligned} \quad (12)$$

and,

$$\begin{aligned} \sigma_{|\cos\theta| \leq a}^{(\pm, \pm)}(\gamma\gamma \rightarrow W^+W^-) &= \frac{2\pi\alpha^2}{s} (3 + \beta_W^2)(1 + 3\beta_W^2) \\ &\quad \left[ \frac{1}{2} \log \frac{1 + a\beta_W}{1 - a\beta_W} + \frac{a\beta_W}{1 - (a\beta_W)^2} \right] , \\ \sigma_{|\cos\theta| \leq a}^{(\pm, \mp)}(\gamma\gamma \rightarrow W^+W^-) &= \frac{2\pi\alpha^2}{s} \left[ 6a\beta_W + (5 - \beta_W^2)(7 - 3\beta_W^2) \frac{a\beta_W}{1 - (a\beta_W)^2} \right. \\ &\quad \left. - \frac{9 + 10\beta_W^2 - 3\beta_W^4}{2} \log \frac{1 + a\beta_W}{1 - a\beta_W} \right] . \end{aligned} \quad (13)$$

Here  $\beta_W$  is the velocity of the final  $W$  boson. The center-of-mass energy dependences of the above cross sections can also be found in Figs. 4 and 5. The cross section of this process shows a mild dependence on the helicity set, even if one introduces an angle cut.

## §4 . Polarization Measurement of Photon Beams

The fact that the cross sections of two processes  $\gamma\gamma \rightarrow \ell^+\ell^-$  and  $\rightarrow W^+W^-$  show different dependences on the photon helicities gives us an idea to measure the po-

larizations of the photon beams. We introduce a ratio of these two production cross sections,

$$\mathcal{R}_{\ell/W} \equiv \frac{\sigma_{|\cos\theta|\leq a}(\gamma\gamma \rightarrow \ell^+\ell^-)}{\sigma_{|\cos\theta|\leq a}(\gamma\gamma \rightarrow W^+W^-)} . \quad (14)$$

The  $\sqrt{s}$  dependences of  $\mathcal{R}_{\ell/W}$  for both photon helicity combinations with  $a = 0.9$  are represented in Fig. 6. For a set of partly polarized photon beams the cross section ratio  $\mathcal{R}_{\ell/W}$  is, of course, described as follows,

$$\mathcal{R}_{\ell/W} = \frac{\frac{1+P_1P_2}{2}\sigma_{|\cos\theta|\leq a}^{(\pm,\pm)}(\gamma\gamma \rightarrow \ell^+\ell^-) + \frac{1-P_1P_2}{2}\sigma_{|\cos\theta|\leq a}^{(\pm,\mp)}(\gamma\gamma \rightarrow \ell^+\ell^-)}{\frac{1+P_1P_2}{2}\sigma_{|\cos\theta|\leq a}^{(\pm,\pm)}(\gamma\gamma \rightarrow W^+W^-) + \frac{1-P_1P_2}{2}\sigma_{|\cos\theta|\leq a}^{(\pm,\mp)}(\gamma\gamma \rightarrow W^+W^-)} , \quad (15)$$

or more simply, neglecting  $\sigma_{|\cos\theta|\leq a}^{(\pm,\pm)}(\gamma\gamma \rightarrow \ell^+\ell^-)$ ,

$$\mathcal{R}_{\ell/W} \simeq \frac{\frac{1-P_1P_2}{2}\sigma_{|\cos\theta|\leq a}^{(\pm,\mp)}(\gamma\gamma \rightarrow \ell^+\ell^-)}{\frac{1+P_1P_2}{2}\sigma_{|\cos\theta|\leq a}^{(\pm,\pm)}(\gamma\gamma \rightarrow W^+W^-) + \frac{1-P_1P_2}{2}\sigma_{|\cos\theta|\leq a}^{(\pm,\mp)}(\gamma\gamma \rightarrow W^+W^-)} , \quad (16)$$

where  $P_1, P_2$  are each *average* polarization of two photon beams 1 and 2 under the condition  $z \geq z_{\text{cut}}$ . The  $P_1P_2$  dependences of  $\mathcal{R}_{\ell/W}$  at several values of  $\sqrt{s}$  are plotted in Fig. 7. The ratio  $\mathcal{R}_{\ell/W}$  is roughly proportional to  $1 - P_1P_2$ , because the denominator in Eq. (16) is not so variant against a change of the colliding photon helicity combination, as seen in Fig. 5.

In an actual experiment  $\mathcal{R}_{\ell/W}$  can be determined by the event rate of two processes,

$$\mathcal{R}_{\ell/W} = \frac{N_{|\cos\theta|\leq a}(\gamma\gamma \rightarrow \ell^+\ell^-)}{N_{|\cos\theta|\leq a}(\gamma\gamma \rightarrow W^+W^- \rightarrow 4\text{jets})} Br(W \rightarrow 2\text{jets})^2 , \quad (17)$$

where  $N_{|\cos\theta|\leq a}(\gamma\gamma \rightarrow \ell^+\ell^-)$  is the number of events of the lepton pair production within  $|\cos\theta| \leq a$  and  $N_{|\cos\theta|\leq a}(\gamma\gamma \rightarrow W^+W^- \rightarrow 4\text{jets})$  is the number of events of four quark jets via a  $W$  pair production within  $|\cos\theta| \leq a$ . And  $Br(W \rightarrow 2\text{jets})$  is the branching ratio of  $W$  boson decay into two quark jets, which has the value  $\sim 2/3$  in the standard model. Here the reason why we concentrate on the neutrinoless final states is to determine  $z$  by the energy sum of the final states.

The cross sections for the helicity sets  $(\pm, \mp)$  are large enough to measure the polarization product  $P_1P_2$  precisely. For example, photon–photon collisions above  $z_{\text{cut}}$  in an operation of  $1 \text{ fb}^{-1}$  integrated luminosity, corresponding to 1 Snowmass year run, at  $\sqrt{s} = 400 \text{ GeV}$  with 100%  $(\pm, \mp)$  photon beam polarizations would produce about 7,600 lepton pairs for each species, and about 14,600  $W$  pairs decaying into

quark jets at  $a = 0.9$ . As mentioned in §2, the beam polarizations can be regarded as uniform if we adopt an appropriate  $z_{\text{cut}}$  value. Then we can treat whole events altogether in an evaluation of  $P_1 P_2$ , and we obtain the expected statistical error of  $\mathcal{R}_{\ell/W}$  less than  $3 \times 10^{-3}$  for any value of  $P_1 P_2$ . The corresponding maximum statistical error of  $P_1 P_2$  is only 3%.

## §5 . Luminosity Measurement at Photon–Photon Colliders

Due to a wide spread of the colliding  $\gamma\gamma$  invariant mass as seen in Fig. 2(b), one should determine not only the total luminosity, but also the luminosity distribution on the  $\gamma\gamma$  invariant mass.

To monitor the luminosity distribution in an actual experiment, one can use the process with the largest cross section with an angle cut. The integrated luminosity  $\int \mathcal{L}_{\gamma\gamma} dt$  can be evaluated at each  $z$  value,

$$\int \mathcal{L}_{\gamma\gamma} dt = \frac{N_{|\cos\theta| \leq a}(\gamma\gamma \rightarrow W^+W^- \rightarrow 4\text{jets})}{Br(W \rightarrow 2\text{jets})^2 \left[ \frac{1+P_1 P_2}{2} \sigma_{|\cos\theta| \leq a}^{(\pm, \pm)}(\gamma\gamma \rightarrow W^+W^-) + \frac{1-P_1 P_2}{2} \sigma_{|\cos\theta| \leq a}^{(\pm, \mp)}(\gamma\gamma \rightarrow W^+W^-) \right]} . \quad (18)$$

The statistical fluctuation of the number of four-jet events prevails the statistical error of the measured integrated luminosity. It is 8% for a one-day operation and 0.8% for a year operation at  $\sqrt{s} = 400$  GeV, where  $\mathcal{L}_{\gamma\gamma} = 1 \text{ fb}^{-1}$  a year above  $z_{\text{cut}}$  and the standard model branching ratio are assumed. A similar formula can be derived for the lepton pair productions, however the lepton pair productions have the disadvantage in the event rate at  $\sqrt{s} \gtrsim 300$  GeV.

## §6 . Discussions

Our methods presented in the above sections are based on the tree-level cross sections of the standard model without Higgs resonance. As mentioned in §3, the cross sections Eqs. (10)~(13) may be shifted by the radiative corrections, the Higgs contribution, as well as new physics like anomalous  $\gamma WW$ ,  $\gamma\gamma WW$  couplings, new particle resonances or  $W$  boson rescatterings by new strong forces, and so on. Such possibilities must be checked by more detailed physical considerations, including the analyses

of the event topology and comparisons with the theoretical simulations of the new physics. We think that improvements to incorporate these effects into our techniques are trivial and easily performed, if the deviations from the standard model caused by the new physics are not so large. The top pair production can be available without worrying about ambiguities of the gauge self-couplings, however, the cross section is not so large, as seen in Fig. 5.

The technique presented in §4 is *not* measuring each photon polarization  $P_1$  and  $P_2$  independently, but measuring only their product  $P_1 P_2$ . A separate measurement of  $P_1$  and  $P_2$  may be performed through other processes with more complicated final states.

In conclusion, the photon beam polarizations and the luminosity at a photon–photon collider can be measured by looking at of both processes  $\gamma\gamma \rightarrow \ell^+\ell^-$  and  $\gamma\gamma \rightarrow W^+W^-$ . It is shown that the beam polarization product and the luminosity can be measured within a sufficiently short time with a good accuracy. We believe that the methods proposed in this paper will be powerful tools to understand the photon beam features at future  $\gamma\gamma$  colliders.

## Acknowledgments

We would like to acknowledge valuable discussions with Drs. Hirotomo IWASAKI, Akiya MIYAMOTO and Toshiaki TAUCHI.

## References

- [1] I. F. Ginzburg, G. L. Kotkin, V. G. Serbo and V. I. Tel'nov, *Pis'ma Zh. Eksp. Teor. Fiz.*, **34** (1981) 514 [*JETP Lett.*, **34** (1982) 491]; *Nucl. Instrum. Methods*, **205** (1983) 47.
- [2] I. F. Ginzburg, G. L. Kotkin, S. L. Panfil, V. G. Serbo and V. I. Telnov, *Nucl. Instrum. Methods Phys. Res.*, **219** (1984) 5.  
V. I. Telnov, *Nucl. Instrum. Methods Phys. Res.*, **A294** (1990) 72.  
I. Endo, *Proc. of the Second Workshop on Japan Linear Collider (JLC)*, KEK, November 6–8, 1990, pp. 323, ed. S. Kawabata, KEK Proceedings 91-10 (1991).  
D. L. Borden, D. A. Bauer and D. O. Caldwell, *SLAC preprint*, SLAC-PUB-5715 (1992).
- [3] R. Najima, *Proc. of the Third Meeting on Physics at TeV Energy Scale*, KEK, September 28–30, 1989, pp. 112, ed. K. Hikasa and C. S. Lim, KEK Report 90-9 (1990).  
T. L. Barklow, *SLAC Preprint*, SLAC-PUB-5364 (1990).  
E. E. Boose and G. V. Jikia, *Phys. Lett.*, **275** (1992) 164.
- [4] I. F. Ginzburg, G. L. Kotkin, S. L. Panfil and V. G. Serbo, *Nucl. Phys.*, **B228** (1983) 285.  
E. Yehudai, *Phys. Rev.*, **D44** (1991) 3434.  
S. Y. Choi and F. Schrempp, *DESY Preprint*, DESY 91-155 (1991).
- [5] O. J. P. Éboli, M. C. Gonzalez-Garcia, F. Halzen and S. F. Novaes, *Univ. of Wisconsin – Madison Preprint*, MAD/PH/701, IFT-P.014/92 (1992).  
J. H. Kühn, E. Mirkes and J. Steegborn, *Universität Karlsruhe Preprint*, TTP92-28 (1992).  
E. Boos, I. Ginzburg, K. Melnikov, T. Sack and S. Shichanin, *Max-Planck-Institut für Physik Preprint*, MPI-Ph/92-48 (1992).  
M. S. Chanowitz, *Phys. Rev. Lett.*, **69** (1992) 2037.  
A. Goto and T. Kon, *Europhysics Lett.*, **13** (1990) 211; erratum *ibid.*, **14** (1991) 281.  
D. L. Borden *et al.* in Ref. [2].

[6] R. H. Milburn, *Phys. Rev. Lett.*, **10** (1963) 75.  
 F. R. Arutyunyan and V. A. Tumanyan, *Zh. Eksp. Theor. Fiz.*, **44** (1963) 2100.  
 $[Sov. Phys. JETP]$ , **17** (1963) 1412].

[7] I. F. Ginzburg *et al.* in Refs. [1] and [2].

[8] T. Nakanishi, H. Aoyagi, H. Horinaka, Y. Kamiya, T. Kato, S. Nakamura, T. Saka and M. Tsubata, *Phys. Lett.*, **A158** (1991) 345.  
 H. Aoyagi, H. Horinaka, Y. Kamiya, T. Kato, T. Kosugoh, S. Nakamura, T. Nakanishi, S. Okumi, T. Saka, M. Tawada and M. Tsubata, *Phys. Lett.*, **A167** (1992) 415.  
 T. Murayama, E. L. Garwin, R. Prepost, G. H. Zapalac, J. S. Smith and J. D. Walker, *Phys. Rev. Lett.*, **66** (1991) 2376.

[9] *Proc. of the Second Workshop on Japan Linear Collider (JLC)*, KEK, November 6–8, 1990, edited by S. Kawabata, KEK, Proceedings 91-10 (1991).  
 S. Orito, *Univ. of Tokyo, ICEPP preprint*, UT-ICEPP 92-05 (1992).  
*Proc. of the International Workshop on Next-Generation Linear Colliders*, Stanford, California, edited by M. Riordan, *SLAC preprint*, SLAC-335 (1988).  
 R. Ruth, *SLAC preprint*, SLAC-PUB-5406 (1991).  
 T. Weiland, to appear in *Proc. of the 1991 Conference on Physics at Linear Colliders*, Saariselka, Finland.  
*Proc. of the First International TESLA Workshop*, Ithaca, New York, edited by H. Padamsee, *Cornell preprint*, CLNS-90-1029 (1990).  
 P. B. Palmer, *Ann. Rev. Nucl. Part. Sci.*, **40** (1990) 529.

[10] An essentially equivalent formula of the differential cross section of fermion pair production from the polarized photons can be found in T. L. Barklow in Ref. [3].

[11] A formula of the differential cross section on Mandelstam  $t$  variable of  $W$  pair production from the polarized photons can be found in I. F. Ginzburg *et al.* in Ref. [4].

## Table

**Table 1:** The luminosity fraction  $\mathcal{F}r$ , the average  $\mathcal{A}v$  of the polarization product  $P_1P_2$  and the minimum  $\mathcal{W}r$  of the polarization product above  $z_{\text{cut}}$  in case of both photon beams are generated by an electron beam with  $P_e = +1.0$  or  $+0.8$ , and a laser beam  $P_L = -1.0$ , at several values of  $z_{\text{cut}}$ . The optimum laser light energy ( $x = 2 + 2\sqrt{2}$ ) is assumed.

$z_{\text{cut}}$	$P_e = +1.0$			$P_e = +0.8$		
	$\mathcal{F}r$	$\mathcal{A}v$	$\mathcal{W}r$	$\mathcal{F}r$	$\mathcal{A}v$	$\mathcal{W}r$
0.80	0.045	0.997	0.985	0.036	0.953	0.913
0.79	0.070	0.991	0.970	0.057	0.936	0.868
0.78	0.095	0.987	0.946	0.078	0.920	0.813
0.77	0.120	0.983	0.911	0.099	0.897	0.747
0.76	0.143	0.974	0.866	0.119	0.877	0.672
0.75	0.164	0.965	0.807	0.138	0.853	0.586
0.74	0.184	0.955	0.736	0.156	0.830	0.492
0.73	0.203	0.943	0.651	0.172	0.805	0.391
0.72	0.220	0.928	0.554	0.188	0.780	0.285
0.71	0.236	0.912	0.447	0.203	0.753	0.176
0.70	0.250	0.896	0.333	0.218	0.726	0.067

## Figure Captions

**Fig. 1** The photon beam spectra (a) and the polarization distributions (b) for the electron beam polarization  $P_e = +1.0$  (solid line),  $+0.8$  (dashed line),  $0.0$  (dotted line) and  $-1.0$  (dot-dashed line). The laser beam polarization is fixed to be  $P_L = -1.0$  for each  $P_e$ , and the optimum laser light energy ( $x = 2 + 2\sqrt{2}$ ) is assumed.

**Fig. 2** A contour plot (a) of the luminosity distribution on the energy fraction  $z$  and the *absolute value* of  $\gamma\gamma$  rapidity  $|\eta|$  for the ideal combination of the electron beam and the laser polarizations  $P_e P_L = -1$ . ‘V’ marks are plotted at the peak point, a local maximum and a local minimum with the code P, H and L, respectively, as well as the value of the distribution at these extremes. Values on the contour lines are  $0.2, 0.5, 0.6$  (two distinct lines),  $1, 2, 5, 10, 20, 50$  and  $100$  from left to right, respectively. The lines of the value  $1, 10$  and  $100$  are dashed and else are dotted. The range  $|\eta| > 1$  is omitted, and the area at right of the bold-solid line is not allowed. Semi-integrated distributions  $1/\mathcal{L}_{\gamma\gamma} d\mathcal{L}_{\gamma\gamma}/dz$  (b) and  $1/\mathcal{L}_{\gamma\gamma} d\mathcal{L}_{\gamma\gamma}/d|\eta|$  (c) are also displayed. The optimum laser light energy ( $x = 2 + 2\sqrt{2}$ ) is assumed.

**Fig. 3** The  $z_{\text{cut}}$  dependences of the luminosity fraction  $\mathcal{F}r$  (a), the average  $\mathcal{A}v$  of the polarization product  $P_1 P_2$  (upper lines in (b)) and the minimum  $\mathcal{W}r$  of the polarization product (lower lines in (b)) above  $z_{\text{cut}}$ . The solid lines correspond to  $P_e = +1.0$ , while the dashed lines are for  $P_e = +0.8$ . The laser beam polarization is fixed to be  $P_L = -1.0$  for each  $P_e$ , and the optimum laser light energy ( $x = 2 + 2\sqrt{2}$ ) is assumed.

**Fig. 4** The C. M. energy dependences of lepton (solid line), quark (dashed line) and  $W$  boson (dot-dashed line) pair production cross sections without the angle cut. The adopted values of c quark, b quark, t quark and  $W$  boson masses are  $1.5, 5, 150$  and  $80$  GeV, respectively. The fine structure constant is fixed to  $1/128$ . Figures (a) and (b) are for the same and the opposite sign photon helicities, respectively. All cross sections are given by the tree-level computations.

**Fig. 5** The C. M. energy dependences of lepton (solid line), quark (dashed line) and  $W$  boson (dot-dashed line) pair production cross sections with an angle cut  $|\cos \theta| \leq 0.9$ . The adopted values of c quark, b quark, t quark and  $W$  boson masses are 1.5, 5, 150 and 80 GeV, respectively. The fine structure constant is fixed to 1/128. Figures (a) and (b) are for the same and the opposite sign photon helicities, respectively. The line corresponds to electron is far below from the figure range in (a). All cross sections are given by the tree-level computations.

**Fig. 6** The C. M. energy dependences of the ratio of pair production cross sections of the lepton and  $W$  boson. The dashed (solid) line is for the same (opposite) sign photon helicities. The  $W$  boson mass is assumed to 80 GeV. Figure (a) is represented in the logarithmic scale, while (b) is in the linear scale. The angle cut  $a = 0.9$  is adopted.

**Fig. 7** The photon beam polarization dependences of the ratio of pair production cross section of the light lepton  $e$  or  $\mu$ , to those of  $W$  boson. The dot-dashed line corresponds to  $\sqrt{s} = 250$  GeV, the bold-solid line 400 GeV, the short dashed line 800 GeV, the dotted line 1200 GeV and the slender-solid line 2000 GeV. The  $W$  boson mass is assumed to 80 GeV. The angle cut  $a = 0.9$  is adopted.

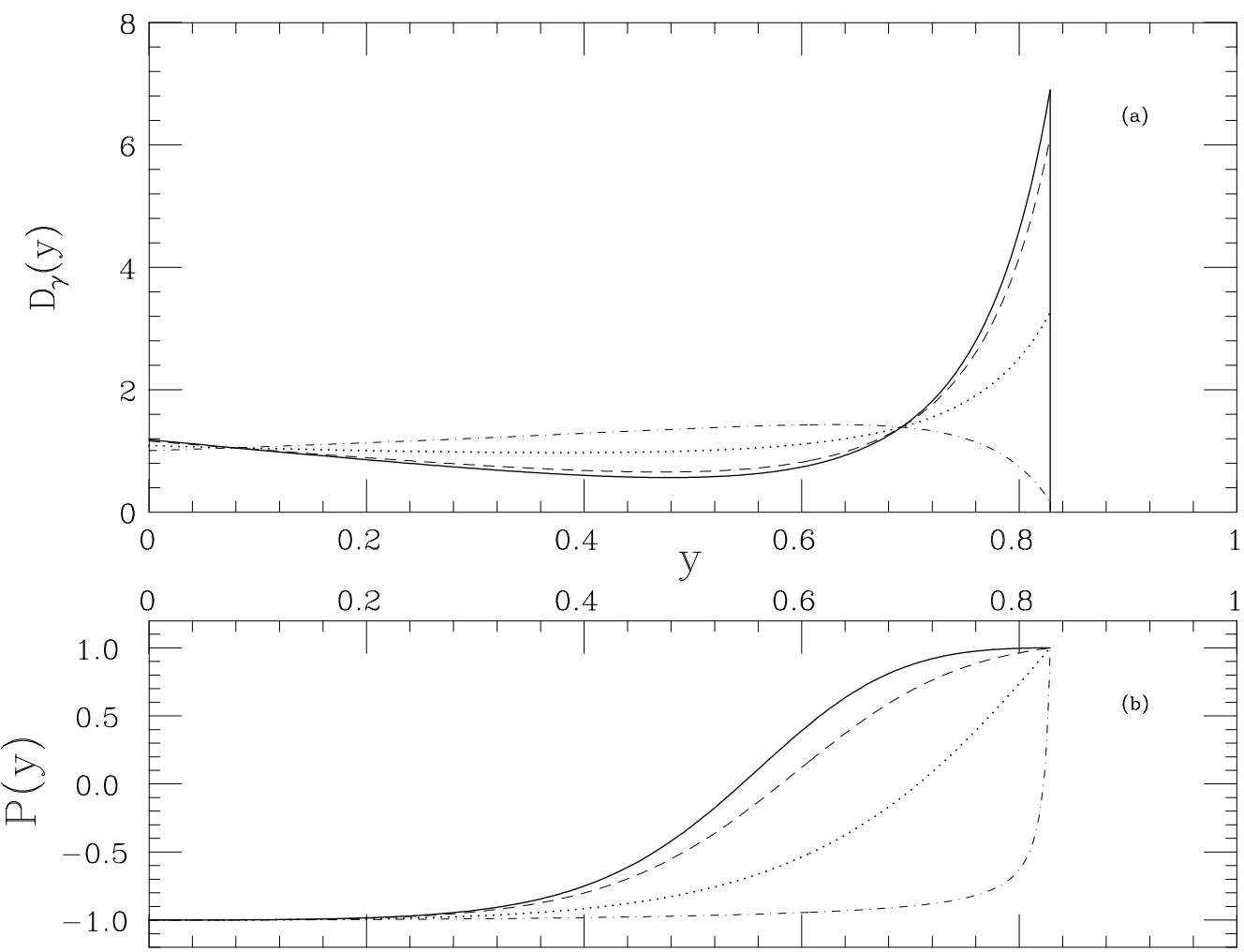
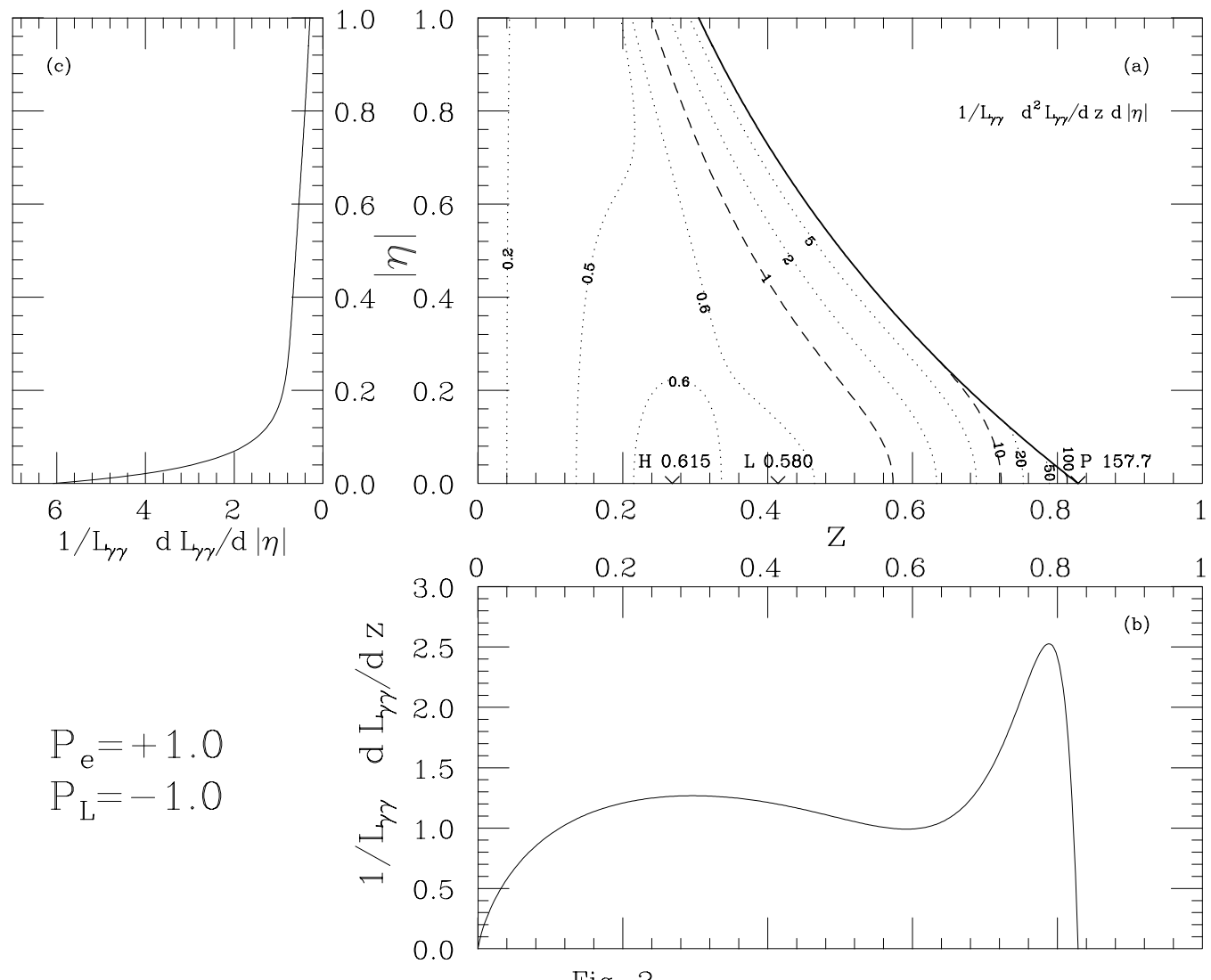


Fig. 1



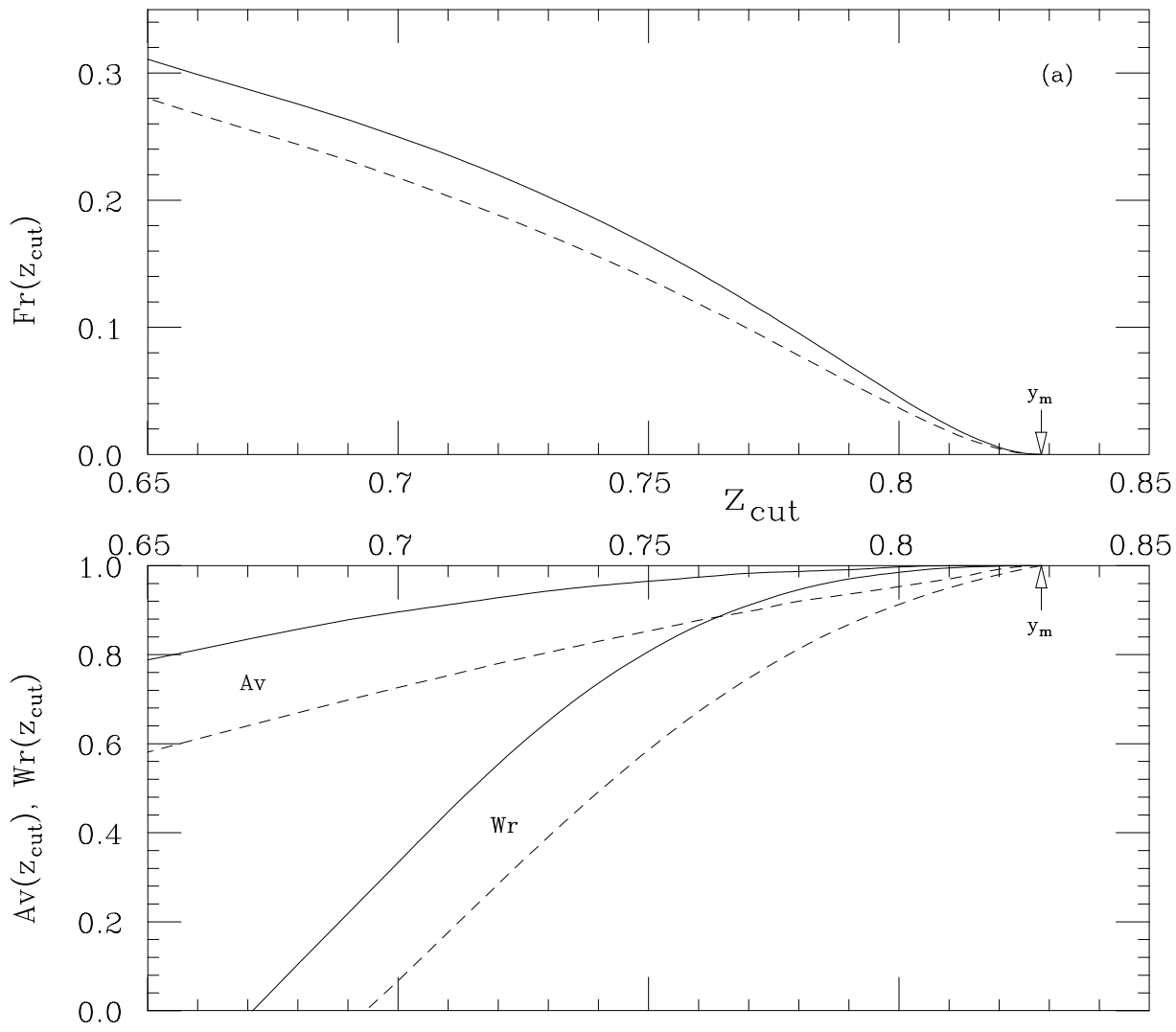


Fig. 3

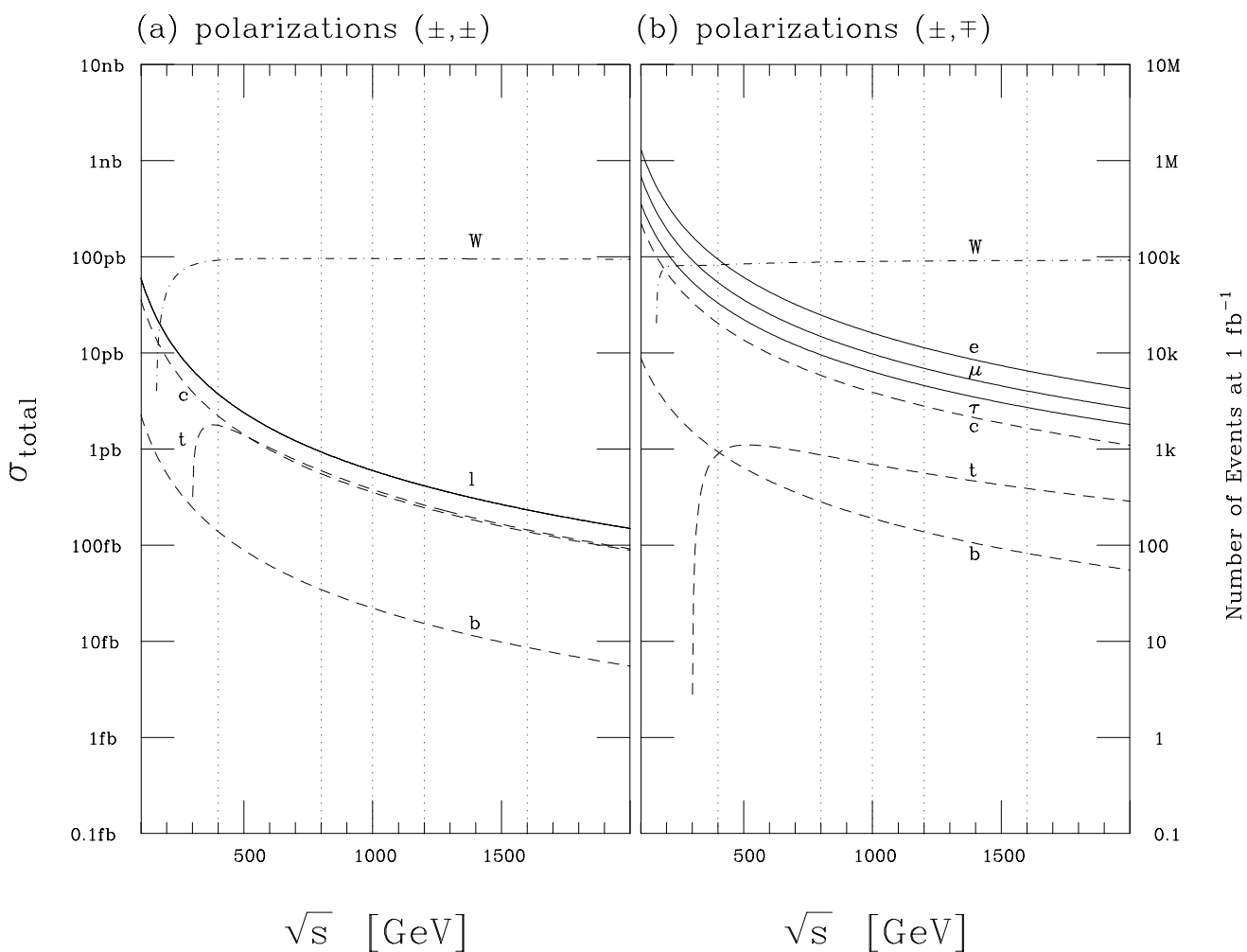


Fig. 4

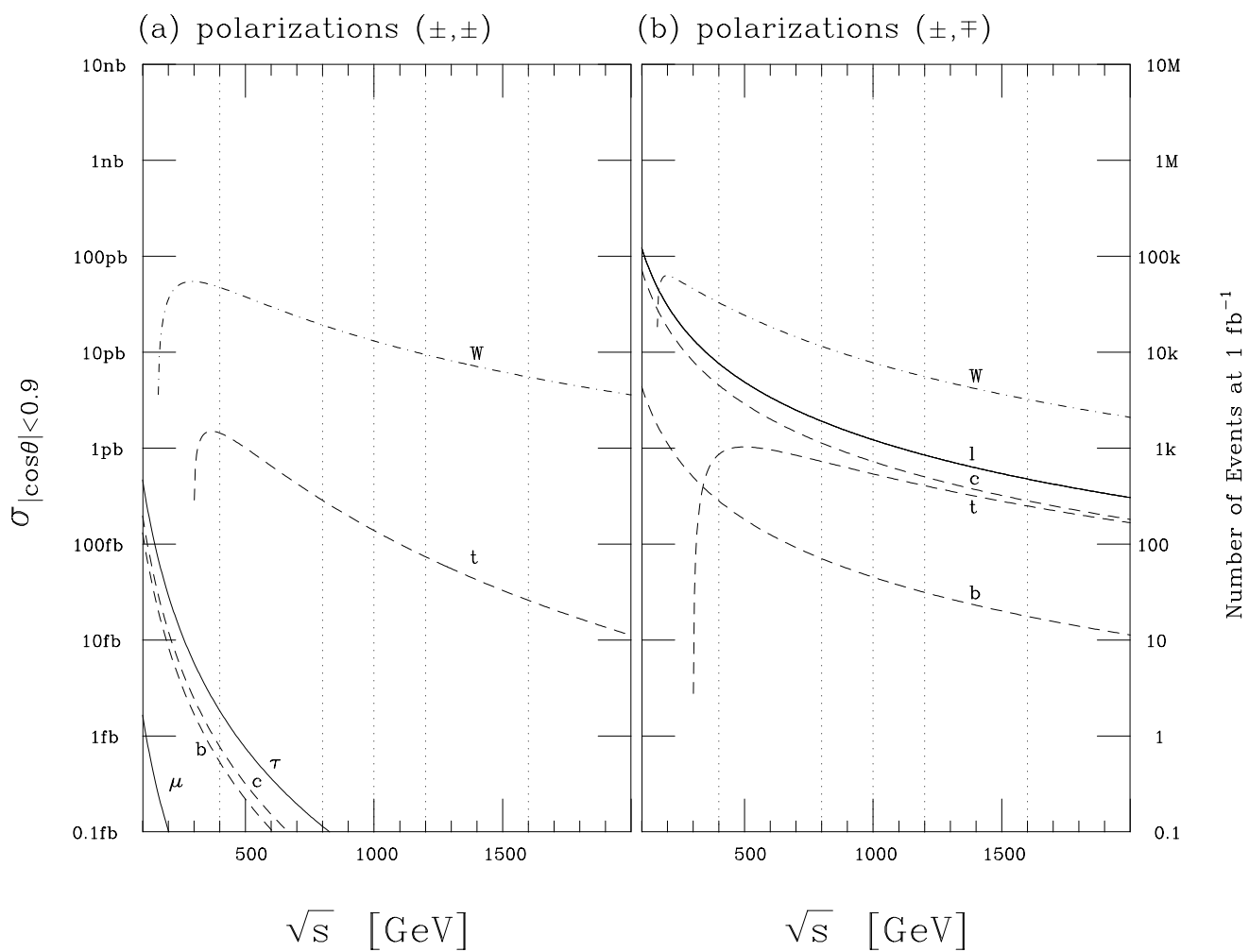


Fig. 5

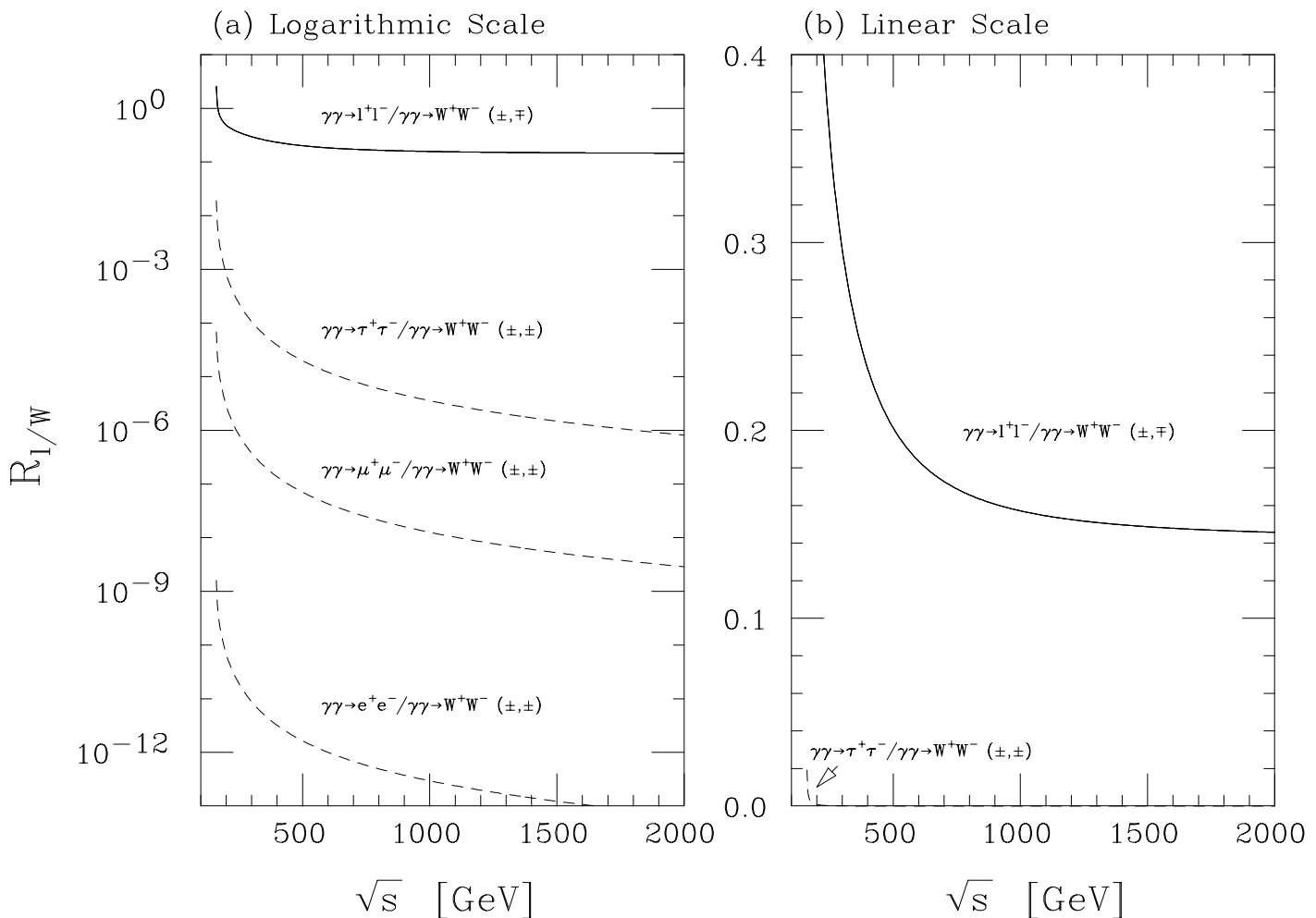


Fig. 6

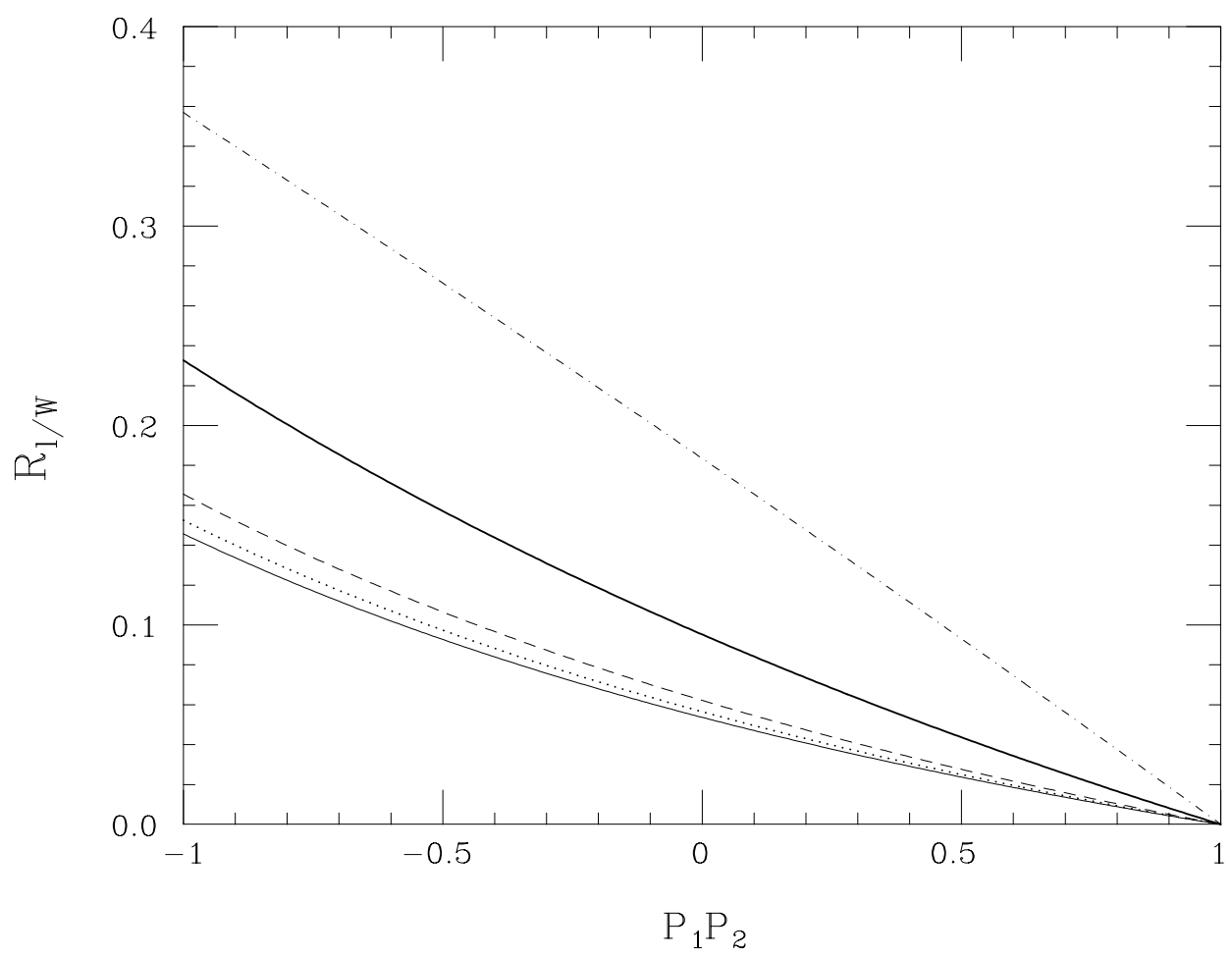


Fig. 7